Fermilab

Fermi National Accelerator Laboratory
P.O. Box 500 • Batavia, Illinois • 60510

TD - 01 - 021
April 05, 2001

An Alternate Mechanical Design and Analysis of FF Arc-Quadrupole for VLHC Stage-2

Deepak Chichili

Abstract

The first version of the mechanical design and analysis of the coil support structure for arc quadrupole was reported in TD-01-012. This report presents an alternate mechanical design and analysis for the coil support structure in which a collar lamination spans 180 degrees. The finite element analysis was carried out for both the magnet straight section and the end cross-section.

1.0 Introduction

An FF arc quadrupole was designed for the VLHC stage 2 operations. The magnet bore diameter is 43.5 mm with a nominal gradient of 400 T/m at 27.2 kA. The design is based on a two-layer Cos (2θ) coil structure made of Rutherford-type Nb_3Sn cable and cold iron yoke. Fig. 1 shows the schematic of the top half of the magnet cross-section. The mechanical support structure consists of 20 mm thick collar laminations made of Nitronic-40. Iron yoke and stainless steel skin surround the collared coil assembly. The collar design is similar to that of LHC arc quadrupole design. A transverse section of the collared coil assembly consists of two laminations covering 180 degrees and two pole inserts in the outer layer pole region not covered by the collars. The collars are mounted by alternating successive set by 90 degrees. In the end regions, round collars are used. This provides continuous support for the coils along the length of the magnet. The collar assembly will be compressed and then locked in place by eight keys. This provides the necessary prestress to the coils. The two collared coil assemblies are then enclosed by two-piece iron yoke, which are radially supported by 5 mm thick stainless steel skin. The yoke is aligned with the collared coils using alignment keys, which maintain some gap between the collars and the yoke laminations. Note that the collars give the entire prestress to the coils and the iron yoke acts only as a flux return. The skin halves are welded under some tension to provide good contact of the iron blocks. Skin alignment keys are installed between the skin shells for the longitudinal magnet alignment.

Finite element analysis using ANSYS was carried out to optimize the coil prestress and to minimize the stress in the collar laminations. It is also important to estimate the magnet cross-section deformation during assembly at room temperature and during excitation at 4.2 K to understand its effect on magnet field quality.

2.0 Finite Element Model: Magnet Straight Section

Since the entire prestress to the coils is provided by the collar structure, each bore can be considered independently for modeling. Further due to symmetry it is sufficient to model quarter section of the bore. The following table lists the thermo-mechanical properties of different materials used in the model:

Material	**E (300 K) GPa**	**E (4.2 K) GPa**	**Poisson's ratio**	**Thermal Contraction K^{-1}**
Coil	38	38	0.3	1.21×10^{-5}
Ground Insulation	14	14	0.3	2.58×10^{-5}
Inner Pole (Al Bronze)	108	113	0.3	1.21×10^{-5}
Wedges (Al Bronze)	108	113	0.3	1.21×10^{-5}
Collar (Nitronic-40)	190	210	0.3	0.90×10^{-5}

Table 1: *Thermo-Mechanical properties of the materials used in the model*.

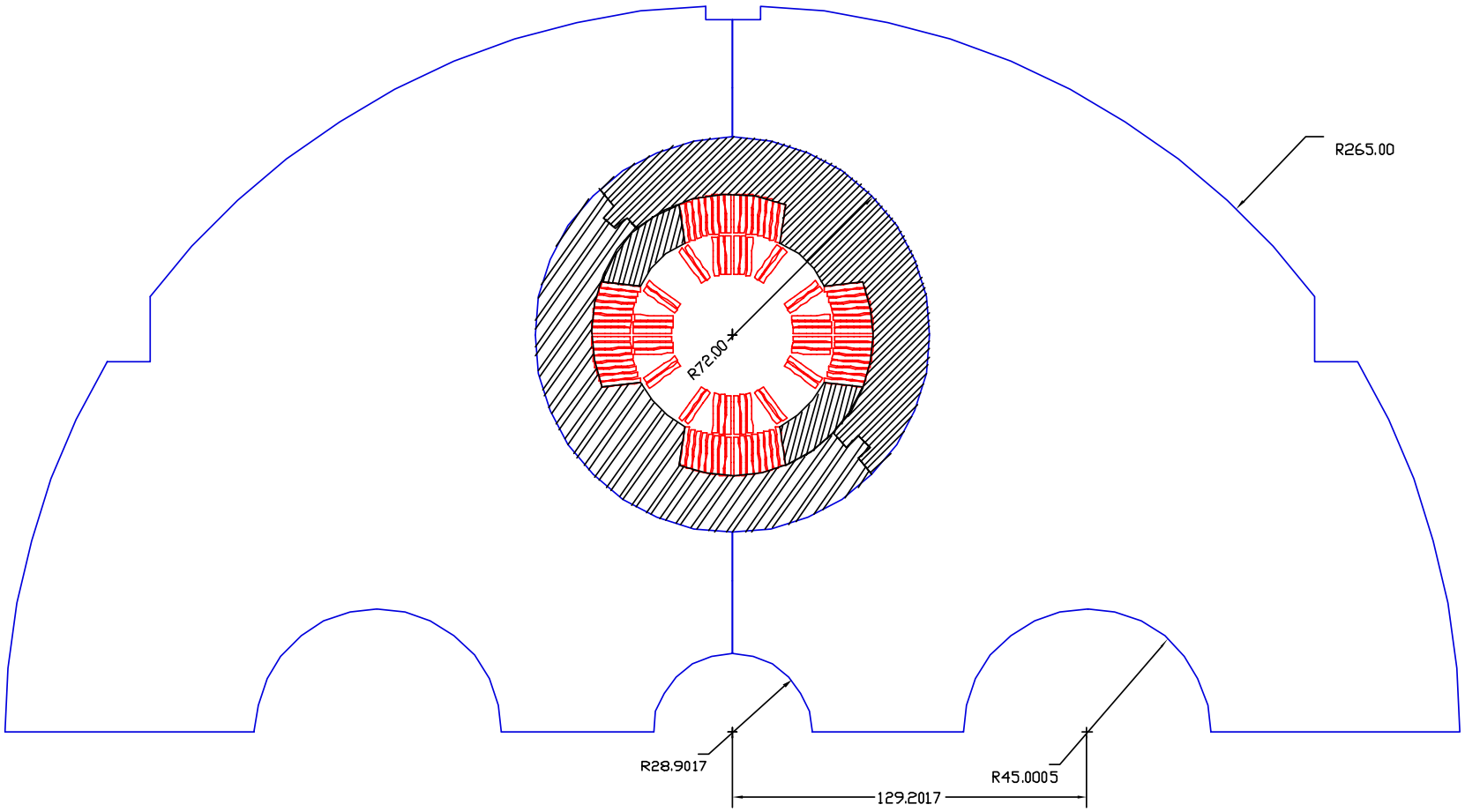

Fig. 1: *Schematic of the coil support structure.*

2.1 Model Description

The model includes inner and outer layer of coils, interlayer and ground insulation, two layers of collar laminations, pole insert and two keys. The inner and outer layers of coils along with the inner pole piece are glued to form a coil structure. The mechanical support structure for the coil assembly consists of two layers. In the first layer we have a collar lamination, which has the in-built pole insert. In the bottom or second layer we have a pole insert and two sets of collar laminations. Two simulate the multi-layer structure of collar laminations in 2D; a 1 mm thick layer was meshed for the coil structure and the keys whereas the collar structure was created by simulating two layers of a 0.5 mm thick mesh. Fig. 2 shows the ANSYS model for the first layer and Fig. 3 shows the ANSYS model with second layer of collar laminations and pole insert on top of the first layer. Note that the plane-stress with thickness option was used. The areas were meshed with two-dimensional elements (Plane 42) and the contact surfaces between collars with CONTACT 48 elements. A friction coefficient of 0.1 was used for CONTACT 48 elements. Having radial interference between the collar structure and the outer layer of coil provided the prestress to the coils. This radial interference was obtained through one-dimensional contact elements, COMBIN 40 oriented perpendicular to the interface. Note that COMBIN 40 elements are frictionless contact elements.

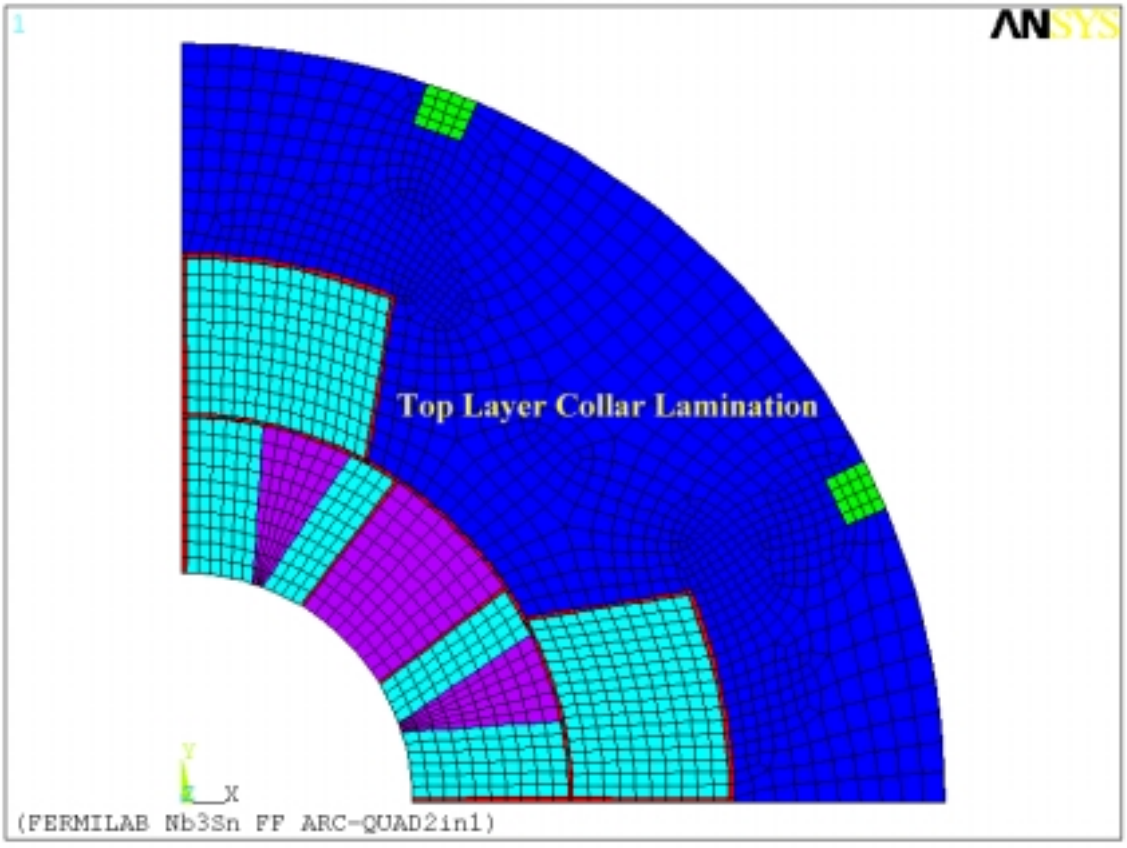

Fig. 2: *ANSYS model showing collared coil cross-section with first layer of collar lamination.*

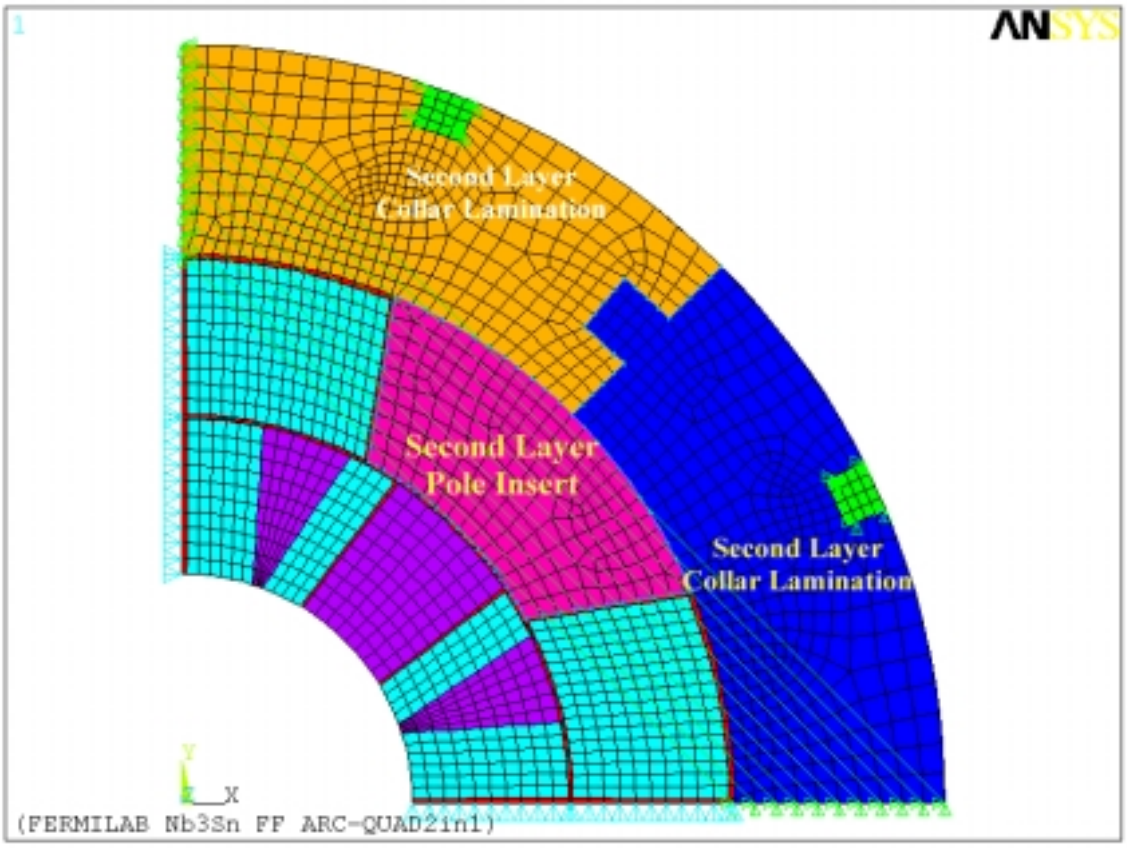

Fig. 3: *ANSYS model showing the collared coil section with the second layer of collar laminations and pole insert shown on top of the first layer of collar lamination. Boundary conditions are also shown in the figure.*

The following are the boundary conditions used in the model; symmetry boundary conditions were used for the coils at 0^o and 90^o. The radial and azimuthal displacements of the front collar at 0^o are coupled to that of the back collar at 90^o. Similarly the radial and azimuthal displacements of the back collar at 0^o are coupled to that of the front collar at 90^o. Finally the front and back collars are coupled to the keys both in the radial and azimuthal directions. Fig. 3 shows the applied boundary conditions.

The first step was to evaluate the Lorentz force distribution in the coils at 27.2 kA, which corresponds to a gradient of 400 T/m. Note that the same mesh for the coil will be used for magnetic and mechanical analysis so that the nodal forces can be easily applied.

2.2 Lorentz Forces

Half section of the coil was first analyzed so that a right geometry of iron yoke can be considered. A quadratic mesh was used in all coil blocks and wedges. Inside each block of coil, the number of elements in azimuthal direction is equal to twice the number of turns. Each coil block is assumed to have a uniform current distribution and the corresponding current density was computed from the current in each cable times the number of turns in

that block. The direction of the current density was applied to reflect the FF configuration of the arc quadrupole. Permeability of iron as a function of magnetic field was used in this analysis. Fig. 4 shows the Lorentz force distribution in the half section of the coil at a gradient of 400 T/m (which corresponds to 27.2 kA of cable current). Table 2 shows the forces in the top quadrant computed with ANSYS and with of OPERA. Fig. 5 shows the flux lines in the magnet cross-section. Note that the direction of the flux lines satisfies the FF configuration of the 2-in-1 arc quadrupole.

Cable Block Number	ANSYS, kN/m		OPERA, kN/m	
	Fx	Fy	Fx	Fy
Block-1	170.491	-829.165	170.175	-832.77
Block-2	486.949	-172.883	485.966	-175.05
Block-3	344.935	-304.006	345.488	-304.86
Block-4	-829.189	169.856	-832.35	169.975
Block-5	-172.915	486.805	-174.998	485.927
Block-6	-304.039	344.789	-304.817	345.495
Total	1002.37	-1306.05		

Table 2: *Lorentz Forces in half- section of the coil.*

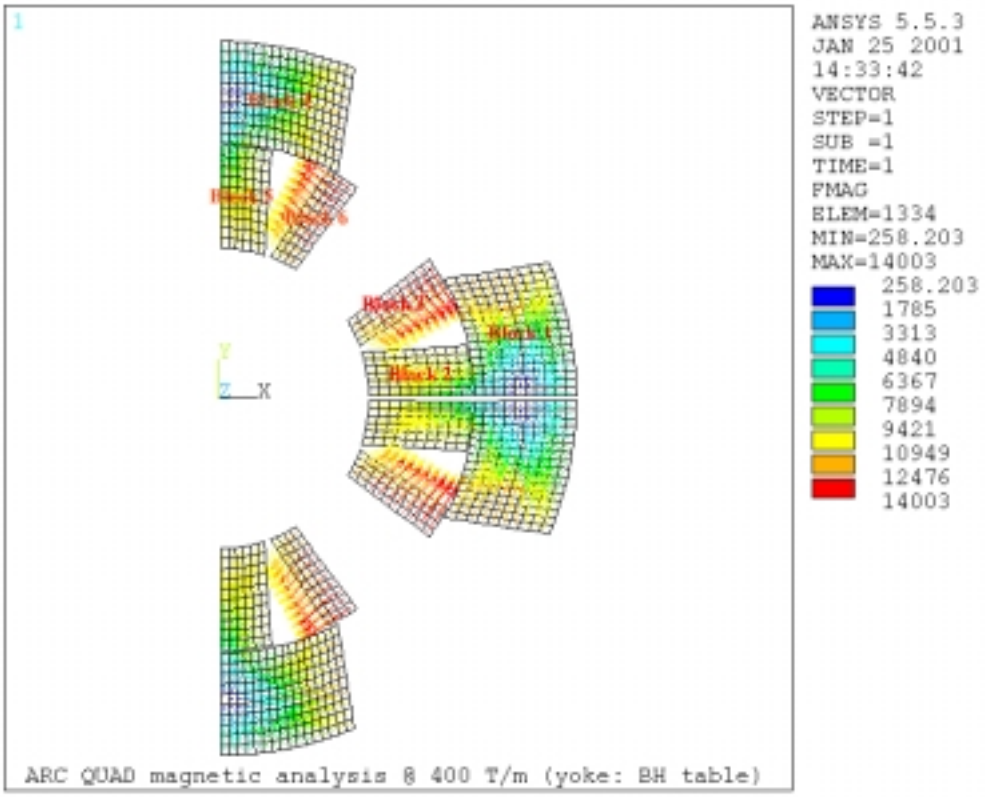

Fig. 4: *Lorentz force distribution in the coil cross-section.*

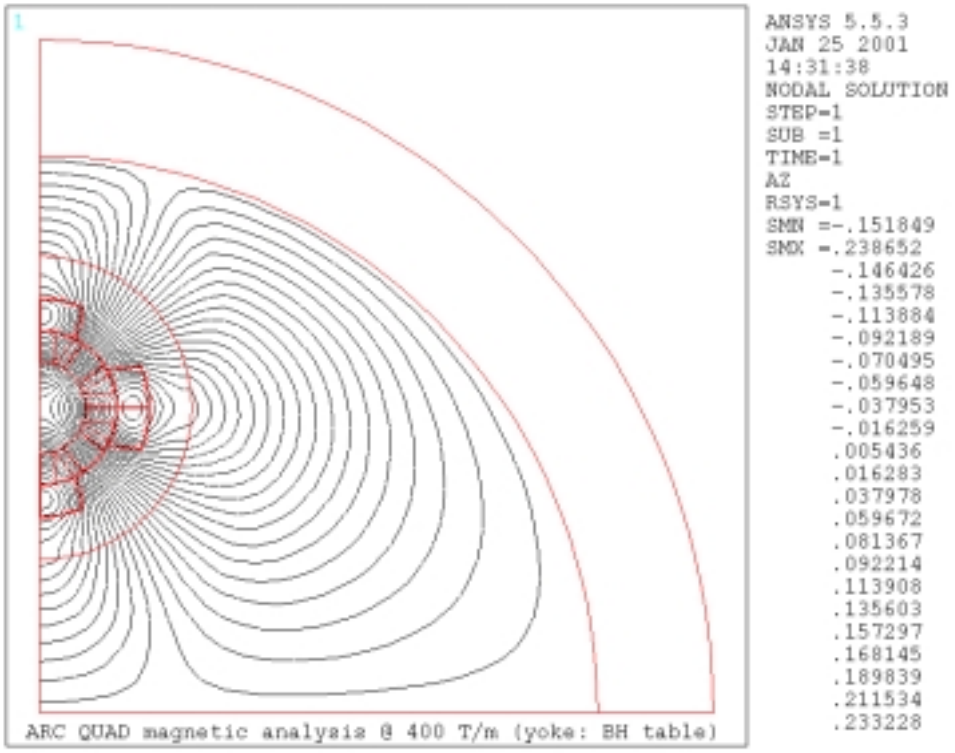

Fig. 5: *Flux distribution in the magnet cross-section.*

2.3 Mechanical Analysis

The interference between the coil and collar determines the amount of prestress in the coils. Typically this is achieved during production through oversize in coil outer diameter. This means an oversized coil is compressed while the keys are inserted into collars. The reaction from the coils force's the collars to expand beyond the nominal loose collar dimensions. The amount of collar deflection is directly proportional to the coil prestress. Hence during magnet production the collar deflection measurements are a good measure to estimate the coil prestress. The goal of this analysis was to find an optimum interference between the coil and the collar laminations.

The acceptable solution should meet the following criteria:

1. The peak stress in the coil should not exceed 150 MPa.
2. A minimum coil stress of 5 MPa at full gradient to ensure that coils do not unload.
3. The maximum collar stress should not exceed the yield stress of the collar material.

After several iterations, the optimum radial interference between the coil and the collar was found to be 0.125 mm. Fig. 6 shows the azimuthal stress distribution in the coil at room temperature after assembly, at 4.2 K and 0 T/m and at 4.2 K and nominal gradient, 400 T/m. The peak stress is about 135 MPa near the inner pole region at room temperature. On the cool down the peak stress in the coil drops to about 100 MPa due to differential thermal contraction between the coil and the Nitronic-40 collar material. Further on excitation, the

peak stress moves to mid-plane due to radial Lorentz forces. Table 3 lists the average azimuthal stress values in the inner and outer coil pole and mid-plane regions during various stages of the magnet. Fig. 7 shows the radial displacement of the coil assembly at various stages of the magnet. Note that the difference in radii between the mid-plane and the pole for the inner bore is only 13 μm at 4.2 K, 0 T/m. At 4.2 K, 400 T/m, the inner bore returns to its circular shape. Table 4 lists the radial displacement of the coil at four different positions (the positions are shown in Fig. 7).

Stages	**Mean Azimuthal Stress, MPa**			
	Inner layer		**Outer Layer**	
	Pole	**Mid-Plane**	**Pole**	**Mid-Plane**
293 K	113	77	5	27
4.2 K, 0 T/m	89	62	3	19
4.2 K, 400 T/m	26	67	6	63

Table 3: *Average azimuthal stress in the coil.*

Stages	**Radial Displacement, μm**			
	Inner layer		**Outer Layer**	
	1	**2**	**3**	**4**
293 K	-53	-40	-65	-74
4.2 K, 0 T/m	-113	-113	-220	-220
4.2 K, 400 T/m	-98	-98	-197	-209

Table 4: *Radial displacements of the coil at four positions.*

The Von-Mises stress distribution in the collar after assembly at room temperature is shown in Fig. 8. The peak stress in the collar is about 700 MPa near the locations where the nodes where coupled to the key. The radial displacements of the collar at various stages of the magnet are shown in Fig. 9 and Table 5 lists the average radial displacements of the collar at mid-plane and pole region. For an average inner layer pole stress of 113 MPa and an outer layer pole stress of 5 MPa (both at room temperature after collaring), the collar deflects by about 57 μm in the mid-plane and 36 μm at the pole. This is equivalent to 1.98 MPa/μm for inner layer pole and 0.09 MPa/μm for outer layer pole with respect to the collar mid-plane displacement.

Stages	**Collar Radial Displacement, μm**	
	Pole	**Mid-Plane**
293 K	36	57
4.2 K, 0 T/m	-162	-151
4.2 K, 400 T/m	-155	-133

Table 5: *Radial displacements of collar.*

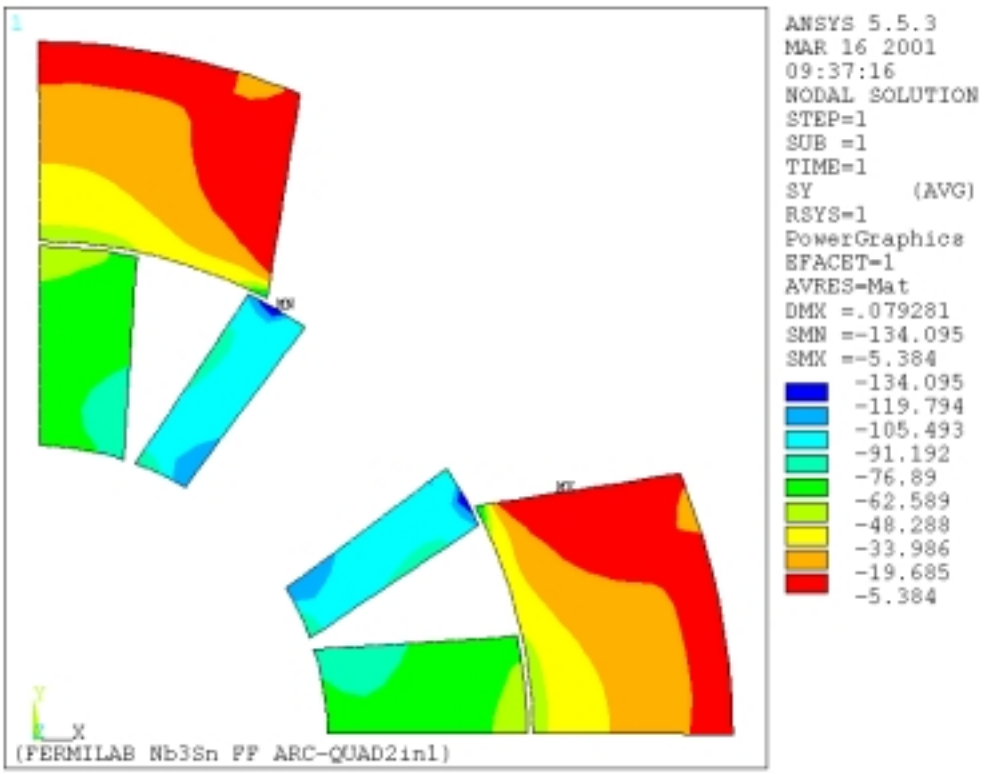

Fig. 6 (a): *Azimuthal stress distribution in the coil at 293 K (after collaring)*

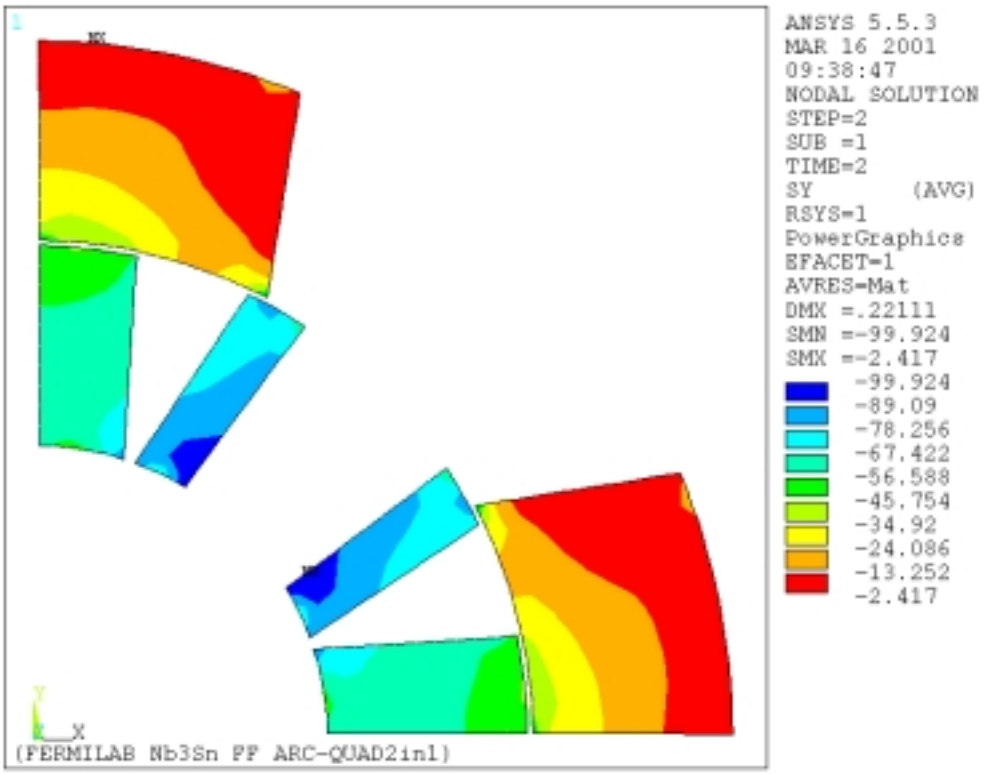

Fig. 6(b): *Azimuthal stress distribution in the coil at 4.2 K, 0 T/m*

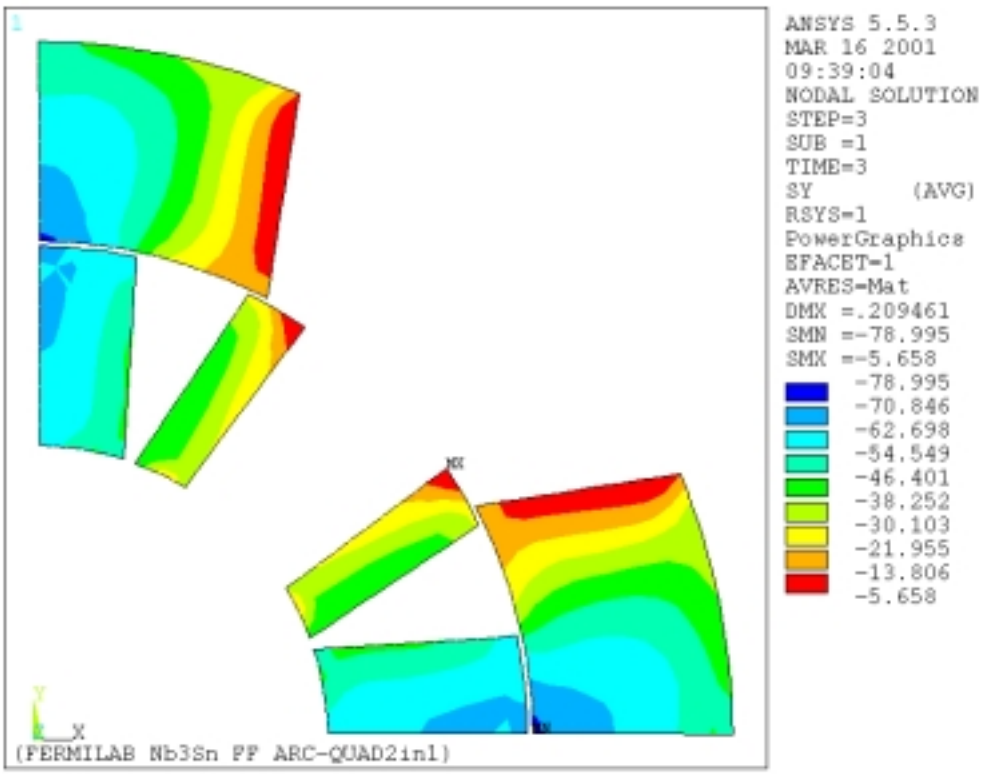

Fig. 6(c): *Azimuthal stress distribution in the coil at 4.2 K, 400 T/m*

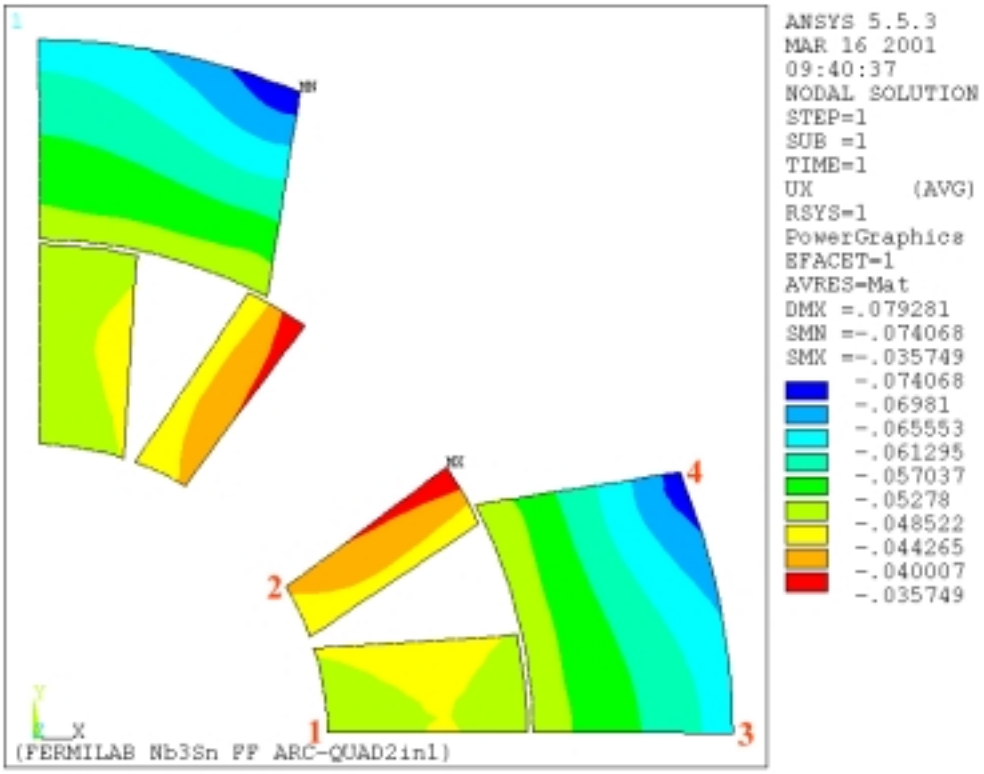

Fig. 7(a): *Radial displacement of the coil at 293 K (after collaring).*

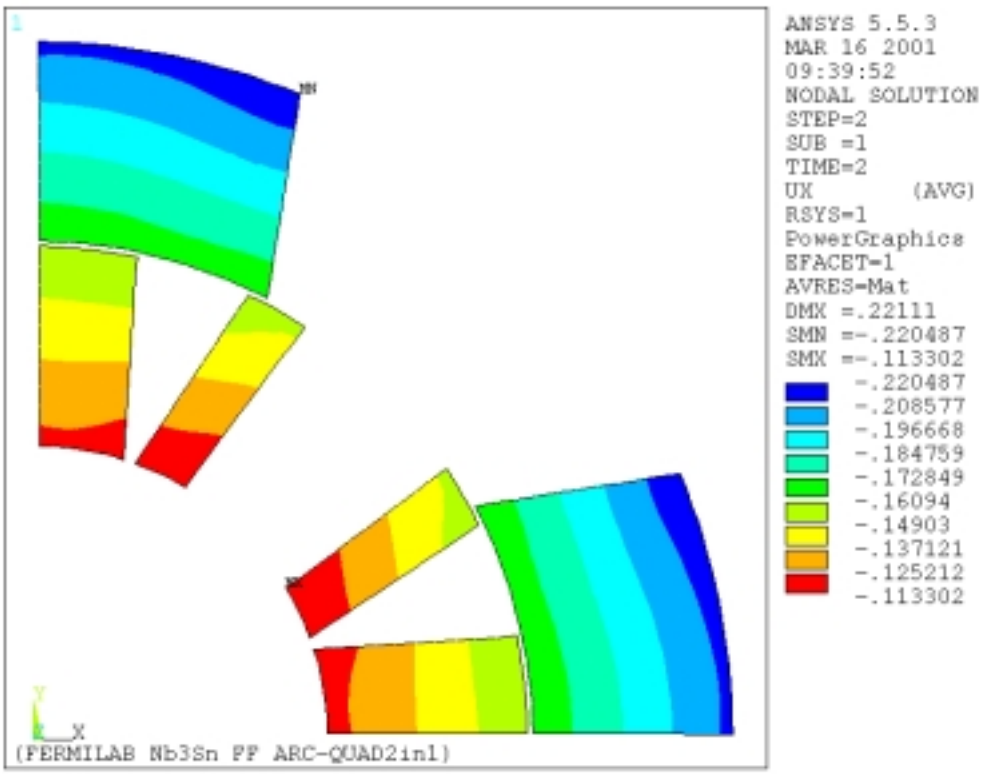

Fig. 7(b): *Radial displacement of the coil at 4.2 K, 0 T/m.*

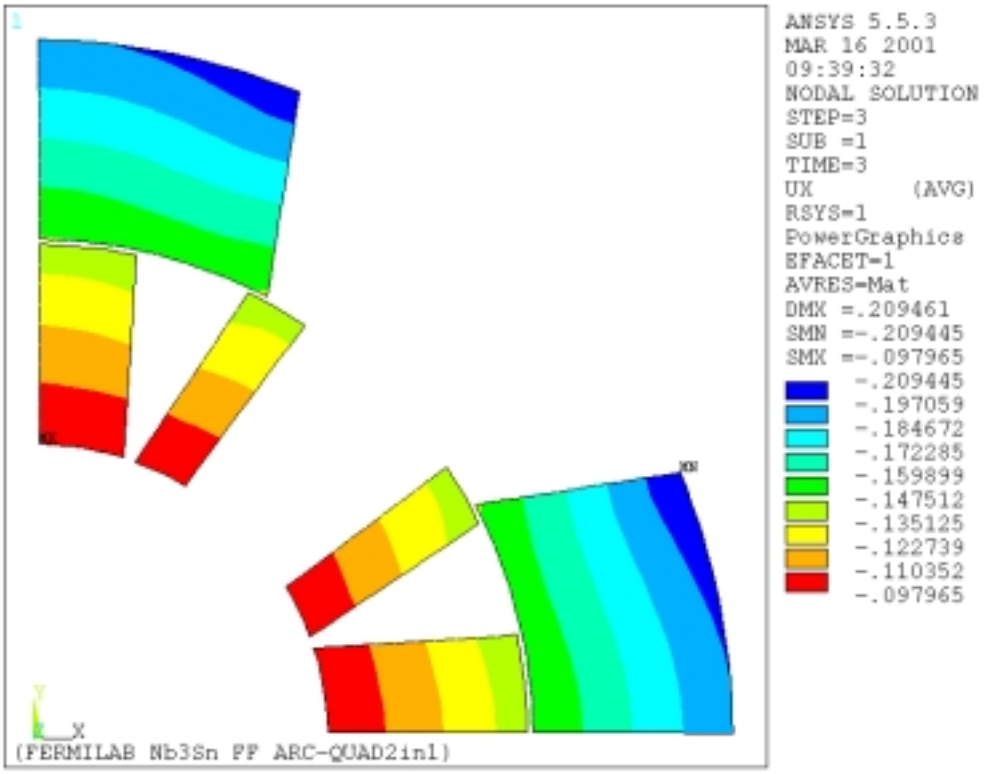

Fig. 7(c): *Radial displacement of the coil at 4.2 K, 400 T/m.*

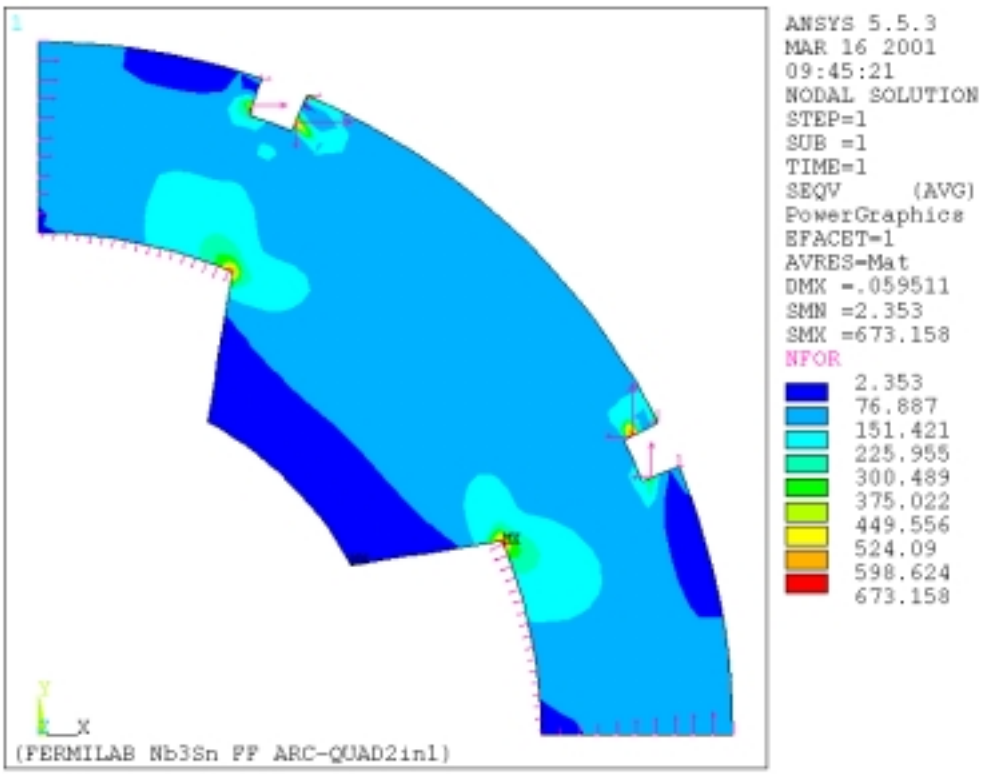

Fig. 8: *Von-Mises stress distribution in the collar after collaring at room temperature.*

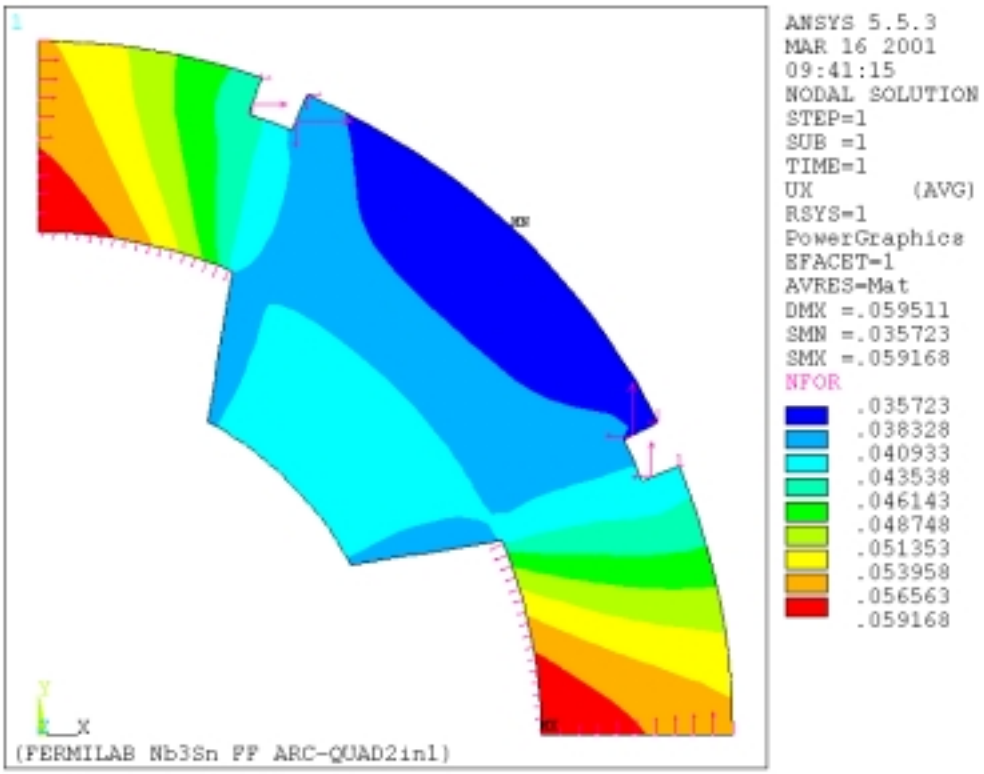

Fig. 9(a): *Radial displacement of the collar at room temperature after collaring.*

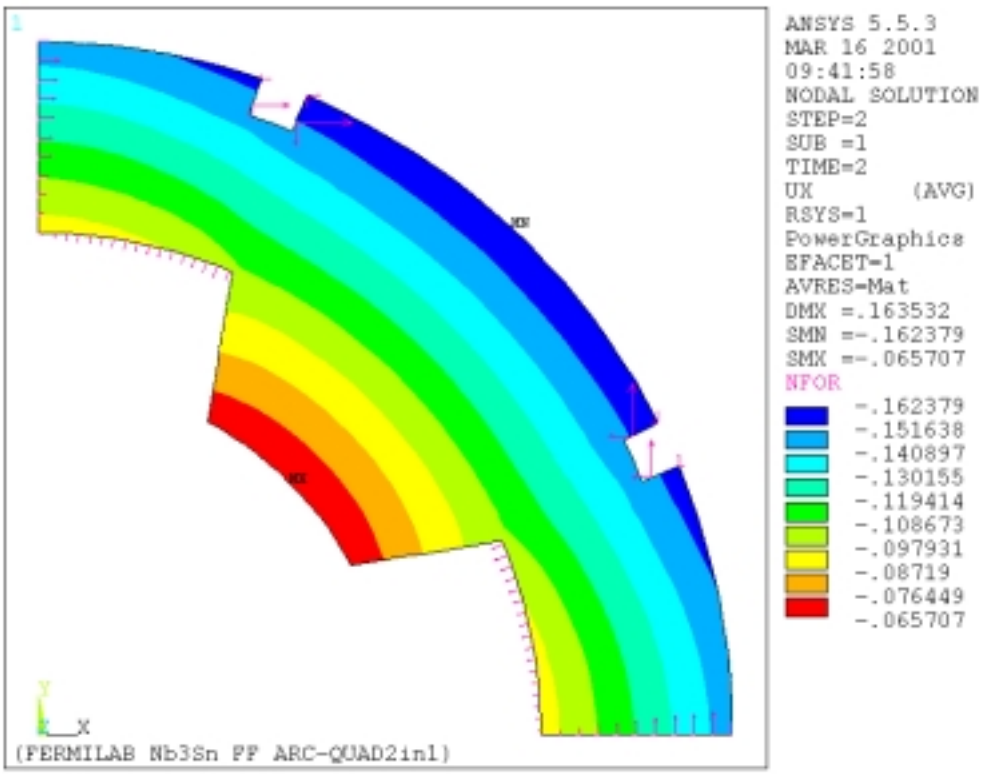

Fig. 9(b): *Radial displacement of the collar at 4.2 K, 0 T/m.*

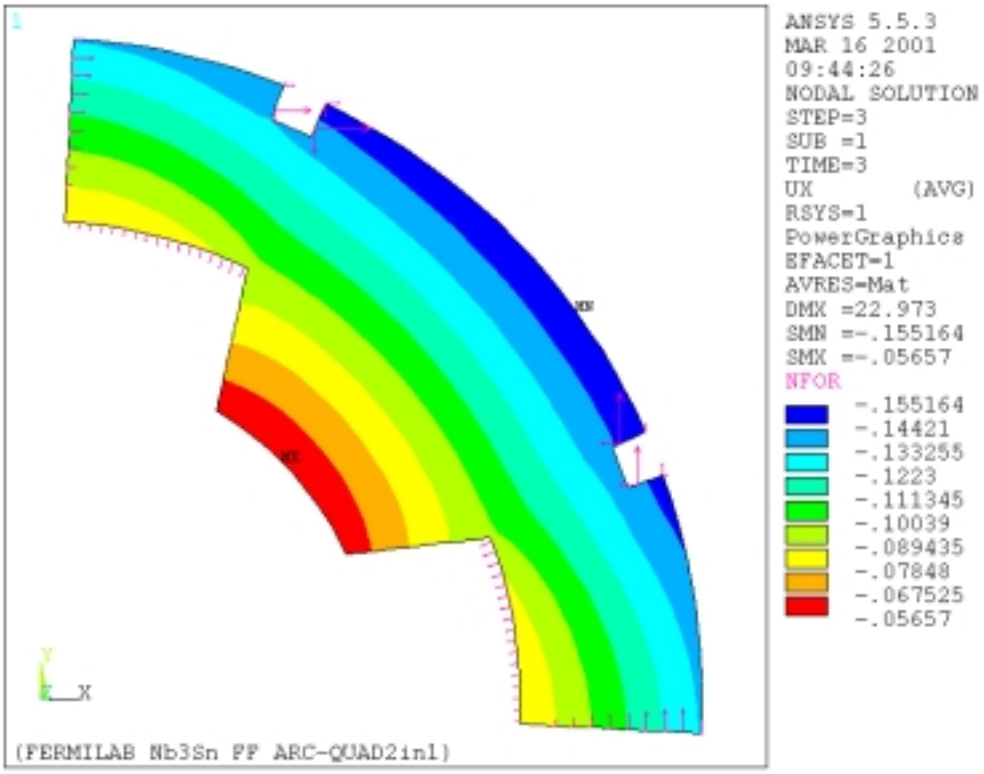

Fig. 9(c): *Radial displacement of the collar at 4.2 K, 400 T/m.*

3.0 Finite Element Model: END CROSS-SECTION

Round collars will be used in the end region as the inner and outer pole pieces are part of the coil structure. Figs. 10 and 11 show the ANSYS end cross-section model of the first layer and second layer of collar structure respectively around the coil.

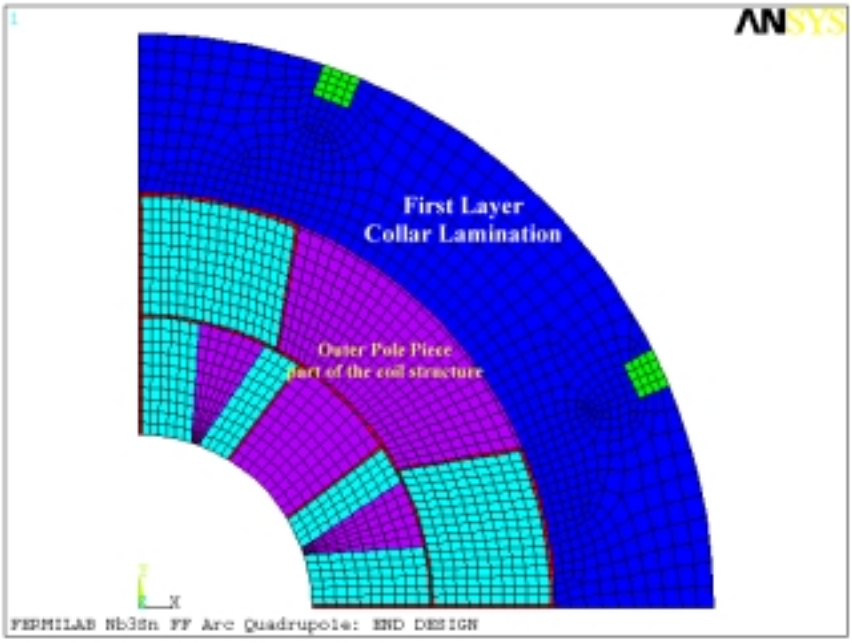

Fig. 10: *ANSYS model of the end cross-section with first layer of collar lamination.*

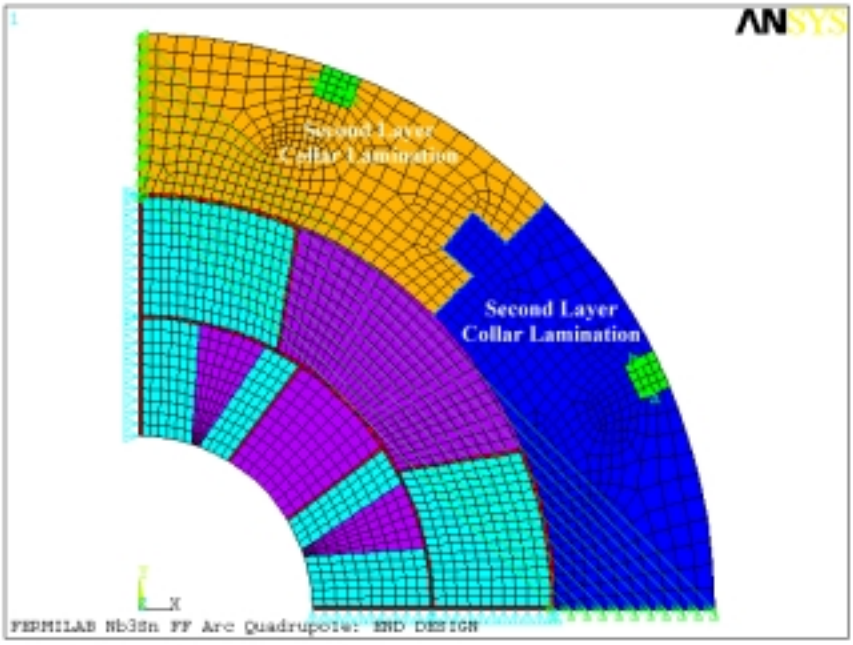

Fig. 11: *ANSYS model of the end cross-section with the second layer of collar lamination shown on top of the first layer.*

The following are the boundary conditions used for this model; symmetry boundary conditions were used for the coils at 0^o and 90^o. The radial and azimuthal displacements of the front collar at 0^o are coupled to that of the back collar at 90^o. Similarly the radial and azimuthal displacements of the back collar at 0^o are coupled to that of the front collar at 90^o. Finally the front and back collars are coupled to the keys both in the radial and azimuthal directions.

After several iterations, the optimum radial interference between the coil and the collar was found to be 0.125 mm, which is similar to that of in the magnet straight section. Fig. 12 shows the azimuthal stress distribution in the coil at room temperature after assembly, at 4.2 K and 0 T/m and at 4.2 K and nominal gradient, 400 T/m. Table 6 lists the average azimuthal stress values in the inner and outer coil pole and mid-plane regions during various stages of the magnet.

Fig. 13 shows the radial displacement of the coil assembly at various stages of the magnet. Table 7 lists the radial displacement of the coil at four different positions (the positions are shown in Fig. 13). Note that the inner bore in the end cross-section remains circular at all stages of the magnet.

Stages	**Mean Azimuthal Stress, MPa**			
	Inner layer		**Outer Layer**	
	Pole	**Mid-Plane**	**Pole**	**Mid-Plane**
293 K	93	93	68	68
4.2 K, 0 T/m	80	69	48	52
4.2 K, 400 T/m	23	87	13	71

Table 6: *Average azimuthal stress in the coil in the end-region.*

Stages	**Radial Displacement, μm**			
	Inner layer		**Outer Layer**	
	1	**2**	**3**	**4**
293 K	-46	-47	-48	-47
4.2 K, 0 T/m	-114	-114	-204	-204
4.2 K, 400 T/m	-98	-98	-199	-199

Table 7: *Radial displacements of the coil at four positions in the end-region.*

The radial displacements of the collar at various stages of the magnet are shown in Fig. 14 and Table 8 lists the average radial displacements of the collar at mid-plane and pole region. For an average inner layer pole stress of 93 MPa and an outer layer pole stress of 68 MPa (both at room temperature after collaring), the collar deflects by about 70 μm in

the mid-plane and 64 μm at the pole. This is equivalent to 1.33 MPa/μm for inner layer pole and 0.97 MPa/μm for outer layer pole with respect to the collar mid-plane displacement.

Stages	Collar Radial Displacement, μm	
	Pole	Mid-Plane
293 K	64	70
4.2 K, 0 T/m	-145	-138
4.2 K, 400 T/m	-144	-136

Table 8: *Radial displacements of the collar in the end-region.*

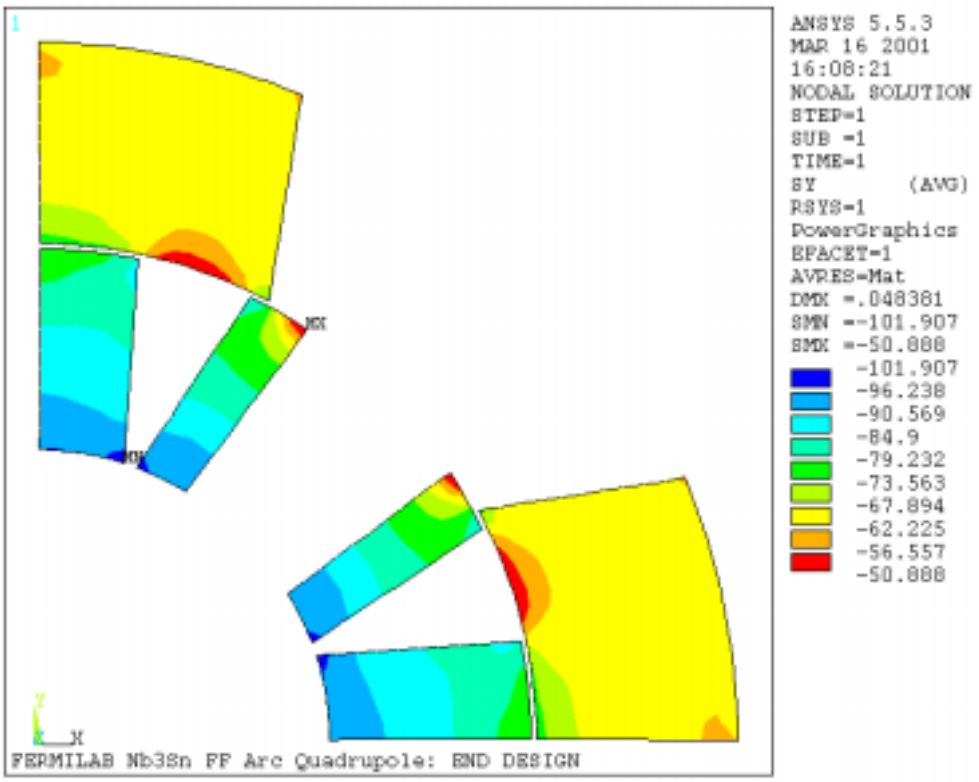

Fig. 12 (a): *Azimuthal stress distribution in the coil end region at 293 K (after collaring)*

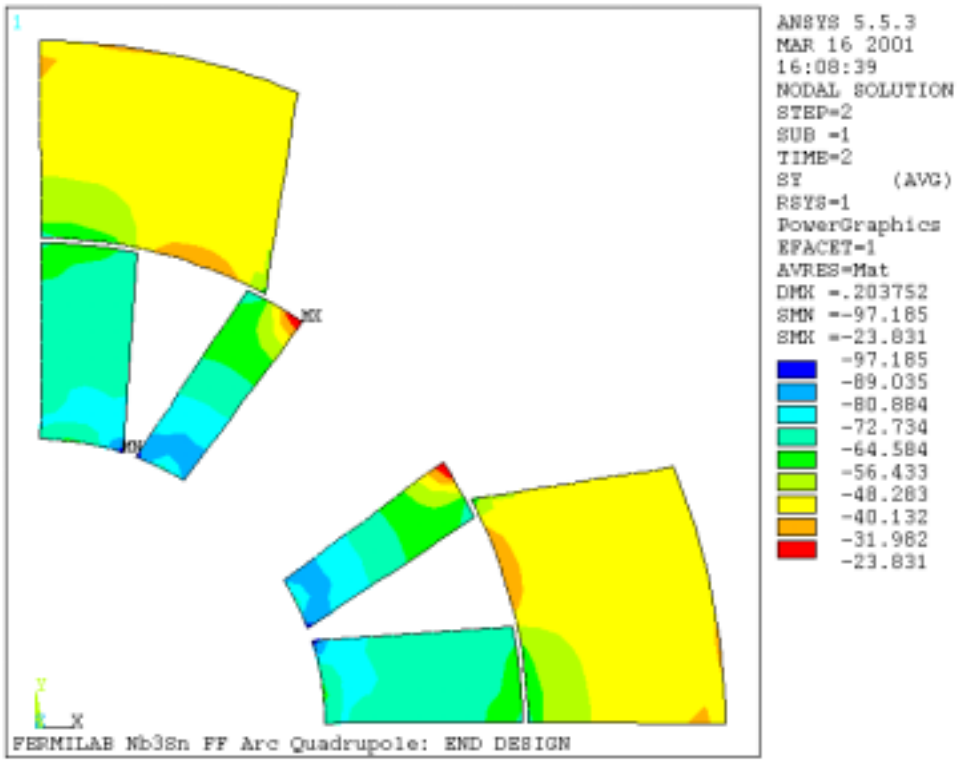

Fig. 12(b): *Azimuthal stress distribution in the coil end region at 4.2 K, 0 T/m*

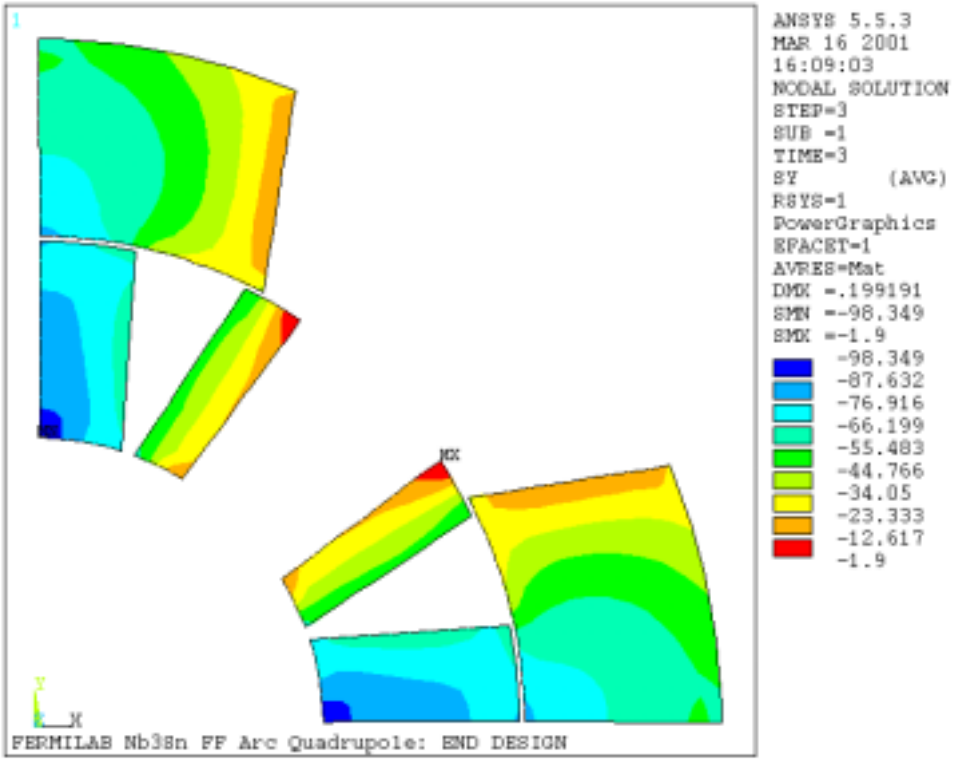

Fig. 12 (c): *Azimuthal stress distribution in the coil end region at 4.2 K, 400 T/m.*

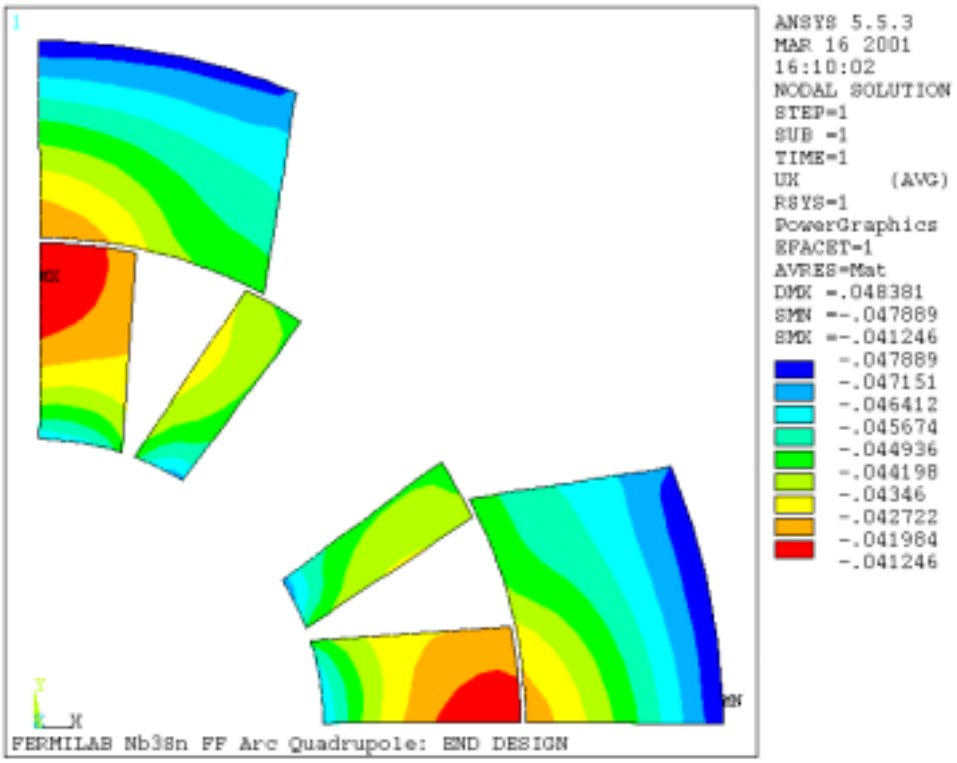

Fig. 13 (a): *Radial displacement of the coil end region at 293 K (after collaring).*

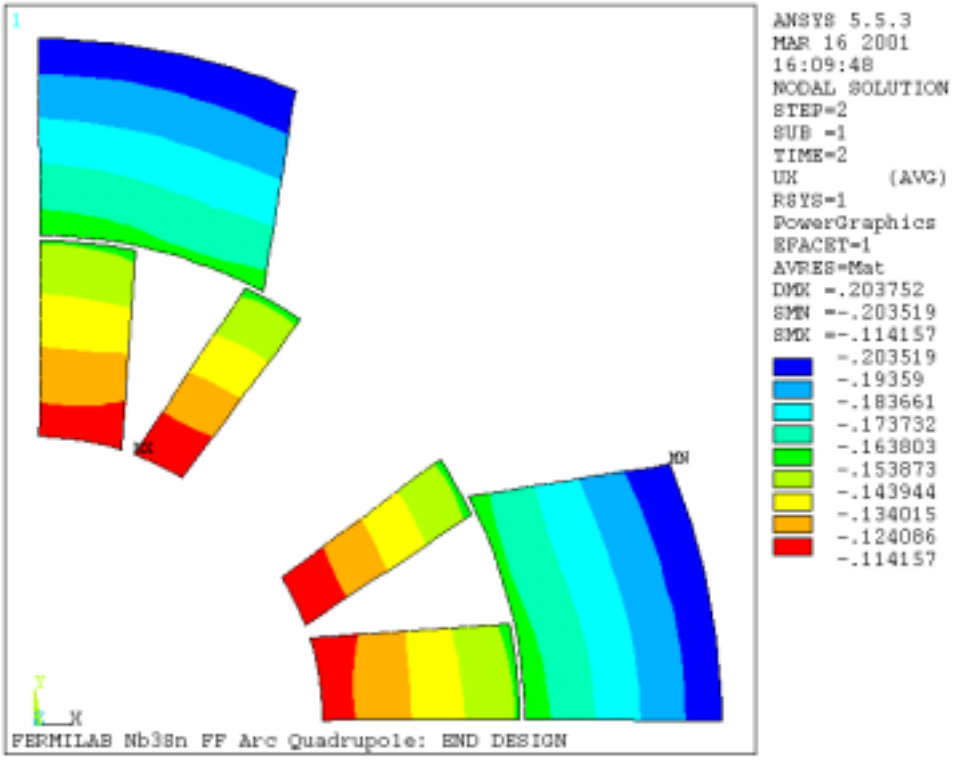

Fig. 13(b): *Radial displacement of the coil end region at 4.2 K, 0 T/m.*

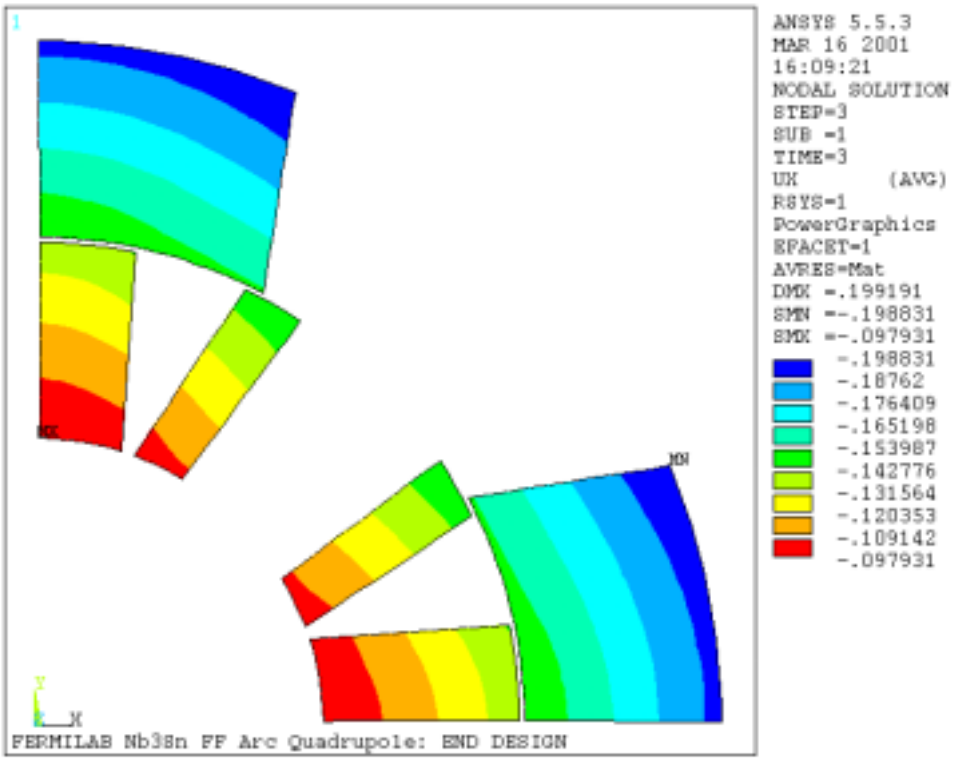

Fig. 13(c): *Radial displacement of the coil at 4.2 K, 400 T/m.*

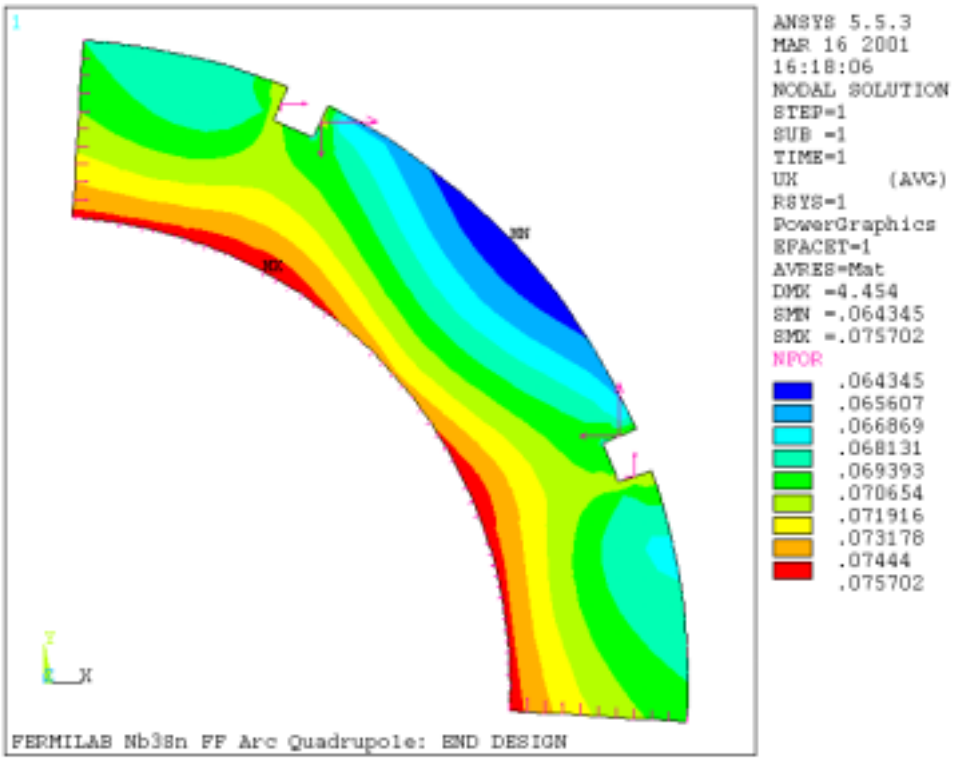

Fig. 14(a): *Radial displacement of the collar lamination in end region after assembly.*

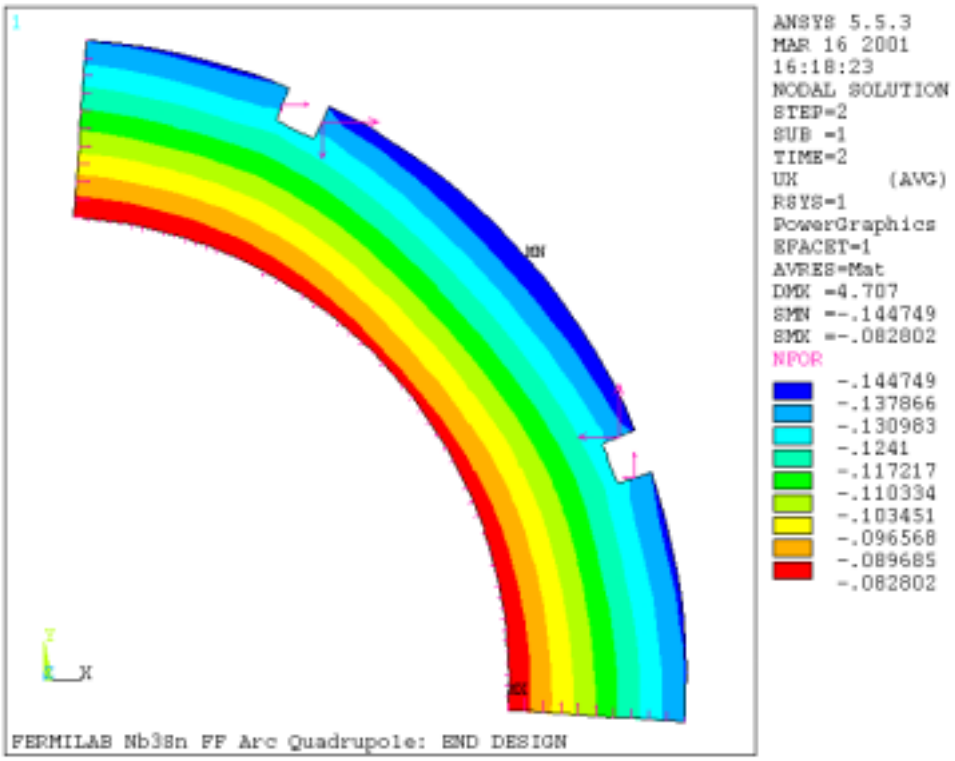

Fig. 14(b): *Radial displacement of the collar lamination in the end region at 4.2 K, 0 T/m.*

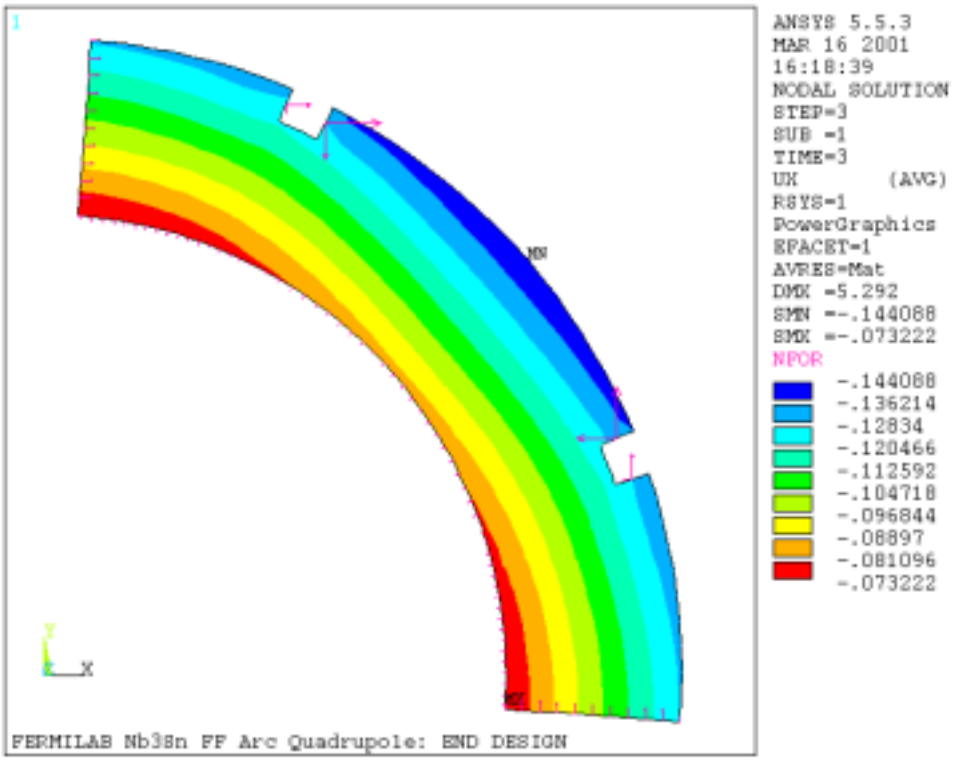

Fig. 14 (c): *Radial displacement of the collar lamination in end region at 4.2 K, 400 T/m.*